

GA-A24537

**OBSERVATION OF MHD INSTABILITY AND
DIRECT MEASUREMENT OF LOCAL PERTURBED
MAGNETIC FIELD USING MOTIONAL STARK
EFFECT DIAGNOSTIC**

by

**R.J. JAYAKUMAR, M.A. MAKOWSKI, S.L. ALLEN,
M.E. AUSTIN A.M. GAROFALO, R.J. LA HAYE,
H. REIMERDES and T.L. RHODES**

NOVEMBER 2003

DISCLAIMER

This report was prepared as an account of work sponsored by an agency of the United States Government. Neither the United States Government nor any agency thereof, nor any of their employees, makes any warranty, express or implied, or assumes any legal liability or responsibility for the accuracy, completeness, or usefulness of any information, apparatus, product, or process disclosed, or represents that its use would not infringe privately owned rights. Reference herein to any specific commercial product, process, or service by trade name, trademark, manufacturer, or otherwise, does not necessarily constitute or imply its endorsement, recommendation, or favoring by the United States Government or any agency thereof. The views and opinions of authors expressed herein do not necessarily state or reflect those of the United States Government or any agency thereof.

OBSERVATION OF MHD INSTABILITY AND DIRECT MEASUREMENT OF LOCAL PERTURBED MAGNETIC FIELD USING MOTIONAL STARK EFFECT DIAGNOSTIC

by

**R.J. JAYAKUMAR,* M.A. MAKOWSKI,* S.L. ALLEN,*
M.E. AUSTIN,† A.M. GAROFALO,◇ R.J. LA HAYE,
H. REIMERDES,◇ and T.L. RHODES‡**

This is a preprint of a paper submitted
to Review of Scientific Instruments.

*Lawrence Livermore National Laboratory, Livermore, California

†University of Texas at Austin, Texas

◇Columbia University, New York

‡University of California Los Angeles, California

Work supported by
the U.S. Department of Energy under
Contract Nos. DE-AC03-99ER54463, W-7405-ENG-48,
and Grant Nos. DE-FG03-97ER54415,
DE-FG02-89ER53297, DE-FG03-01ER54615

**GA PROJECT 30033
NOVEMBER 2003**

ABSTRACT

The local oscillating component of the poloidal magnetic field in plasma associated with MHD instabilities has been measured using the motional Stark effect (MSE) diagnostic on the DIII-D tokamak. The magnetic field perturbations associated with a resistive wall mode (RWM) rotated by internal coils at 20 Hz was measured using the conventional MSE operation mode. These first observations of perturbations due to a MHD mode were obtained on multiple MSE channels covering a significant portion of the plasma and the radial profile of the amplitude of the perturbed field oscillations was obtained. The measured profile is similar to the profile of the amplitude of the electron temperature oscillation measured by electron cyclotron emission (ECE) measurements. In a new mode of measurement, the amplitude of a tearing mode rotating at a high frequency (~ 7 kHz) was observed using the spectral analysis of high frequency MSE data on one channel. The spectrum consists of the harmonics of the light modulation employed in the MSE diagnostics, their mutual beat frequencies and their beat frequencies with the rotation frequency of the tearing mode. The value and time variation of the frequency of the observed perturbations is in good agreement with that measured by Mirnov probes and ECE. The paper demonstrates that the MSE diagnostic can be used for observing low and high frequency phenomena such as MHD instabilities and electromagnetic turbulence.

1. INTRODUCTION

Tokamaks are toroidal plasma devices and the plasma is held in equilibrium with a strong toroidal magnetic field (long around the major radius of the toroid) and a weaker poloidal field (short way around the minor radius of the toroid). These equilibria are characterized by the existence of surfaces on which the poloidal flux is constant. Plasma equilibria are subject to magnetohydrodynamic (MHD) instabilities and plasma turbulence with a range of spatial scales and frequencies. The understanding and control of such instabilities and turbulence in plasma are key to achieving high performance in all fusion devices. The measurement of the structure of these plasma phenomena is necessary for such an understanding. The instabilities have associated perturbations to the local magnetic field and this perturbation is mainly in the poloidal field in tokamaks. Typically, the displacement of the flux surfaces associated with an MHD activity is deduced from the measurement of electron temperature perturbation, e.g., with electron cyclotron emission (ECE) measurements with the assumption that the electron temperature is constant on a flux surface. The structure of the MHD instability is then derived from this deduced quantity and the measurement of the oscillating field outside the plasma boundary using magnetic probes. Measurements along two or more toroidal and poloidal chords are required to identify the mode number and the amplitude if the mode is stationary. However, when plasmas have toroidal rotation and the mode rotates with the plasma, the mode appears to have an oscillating component of poloidal field and the mode characteristics can be obtained from the measurements at a single toroidal location.

While ECE and magnetic probe data are commonly used to deduce the oscillating component of magnetic field, a direct measurement of the perturbed magnetic field in a hot plasma has not been made so far. The measurement of the magnetic field perturbation is a direct measurement of the MHD behavior of the plasma. Such a measurement is also necessary to obviate the need for using plasma theory and models to get a measurement of the magnetic perturbations. On the other hand, the measurements can be used to benchmark plasma models and codes. Such a measurement would, for example, be needed (a) when the ECE diagnostic is not available due to diagnostic limitations or due to density cut off, (b) when the assumption of electron temperature being a flux quantity is not valid due to electrostatic fields or local electron heating, or (c) to check the consistency between the profile of the poloidal flux and its derivative. In this paper, we report the first such direct measurements of the local poloidal field associated with MHD instabilities using the motional Stark effect (MSE) diagnostic, assuming that the period of mode rotation is short compared to time scales of equilibrium changes.

In the example of first measurements using the conventional MSE measurement technique [1–4], the profile of the poloidal field oscillation associated with a rotating resistive wall mode

(RWM) [5] was obtained. Normally, the RWM field is nearly locked to the wall and is detected by the appearance of a non-axisymmetric radial field, e.g., with a saddle coil probe outside the plasma. A recent DIII-D upgrade included installation of active internal coils [6] which can apply helical fields. Application of oscillating currents to these coils provides a resonant rotating field and the RWM is slowly rotated at the imposed frequency [7]. Under this condition, MSE measurements give the poloidal field perturbation associated with the RWM. In the example of the measurement shown in this paper, the radial profile of the perturbed field of a RWM rotated at 20 Hz was obtained from the oscillating component of the pitch angle measured by MSE. The field perturbation is found to be spread over the full plasma radius and has a peak RMS amplitude of 85 G. The profile and the peak value of the perturbed field are consistent with the ECE measurements and the flux surface displacement is in agreement with that deduced from ECE measurements. The intensities of MSE signals can also give a measure of the density oscillation. However, collisional radiative calculations for the observed D_α lines are required and the effect of the density of the neutral beam would need to be characterized for this.

The above method is applicable only in cases where the observed frequency of the oscillating field (proportional to the local rotation frequency) is much smaller than the two modulation frequencies of the photo-elastic modulators (PEM) [8] employed in the MSE diagnostic. Therefore, a different method was developed for the observation and measurement of the n (toroidal mode number) = 1 tearing mode rotating toroidally at the plasma rotation frequency. In this measurement, the MSE data was digitized at a fast rate and the data was spectrally analyzed. The amplitude of the signals at the beat frequencies of the PEM modulation frequency and the mode frequency give the pitch angle associated with perturbed field and the plasma density perturbations. The density perturbations can also be obtained from the signals at the plasma rotation frequency as stated before. This paper describes the demonstration of the technique using one channel of MSE viewing a location at which the tearing mode was present. Measurements with a multi-channel high frequency MSE system are underway to measure the profile of such MHD instabilities. This new technique can be used for any high frequency phenomenon which has associated magnetic field perturbations. The comparison of the results obtained on the perturbed field with that from ECE and wall probe measurements would lead to further characterization of coherent MHD activity and turbulent activity.

2. DIII-D MSE DIAGNOSTIC

The DIII-D tokamak has a 45-channel MSE system in three arrays as shown in Fig. 1. The MSE diagnostic uses the Doppler shifted D_{α} line emitted by the heating beam which is excited by plasma electrons and ions. The D_{α} line is Stark split by the $\mathbf{V} \times \mathbf{B}$ electric field experienced by the beam giving three groups of spectral lines; the central group is polarized perpendicular (σ) to the electric field and the two groups on either side of the spectrum have parallel (π) polarization. The DIII-D system uses the σ polarization. The MSE polarimetry measures the angle of polarization of the σ component with respect to a reference axis and this is related to the plasma magnetic and electric field components by the relation,

$$\tan \gamma = \frac{A_1 B_z + A_5 E_R}{A_2 B_t + A_3 B_R + A_4 B_z + A_6 E_z + A_7 E_R}, \quad (1)$$

where the A coefficients depend on the beam energy, viewing and beam geometries and the subscripts r,z and t refer to radial, vertical and toroidal directions. The spatial overlap of different view chords with different A coefficients permits determination of different field components. For the DIII-D tokamak, the DIII-D view chords are in the median plane ($z \sim 0$), so that the radial magnetic field is usually small and under typical tokamak operating conditions, E_z is also small. Therefore, to the zeroth order, the measured MSE pitch angle is proportional to B_z/B_t and the radial electric field is a correction, which can be significant for certain plasma conditions, particularly at the plasma edge.

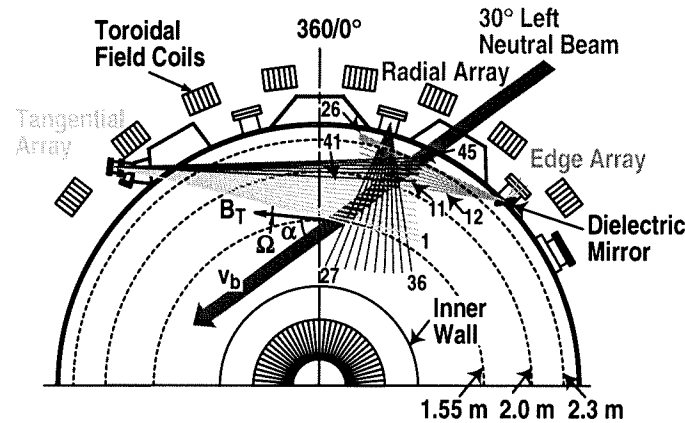


Fig. 1. Forty-five channel MSE system showing three arrays.

The MSE optics gather the light emitted from the beam, which is focused by an objective lens system and then passes through an optical window and a pair of PEMs (Fig. 2). Each PEM

modulates the polarization of the light at a different frequency. The polarization modulation is converted into an amplitude modulation by a linear polarizer, yielding a time dependent intensity [1]

$$I_{\text{tot}} \sim I_{\text{bk}} + I_{\sigma} + I_{\pi} + \frac{I_{\sigma} - I_{\pi}}{\sqrt{2}} [\cos(2\omega_1 t) \sin(2\gamma) + \cos(2\omega_2 t) \cos(2\gamma)] + \dots \quad (2)$$

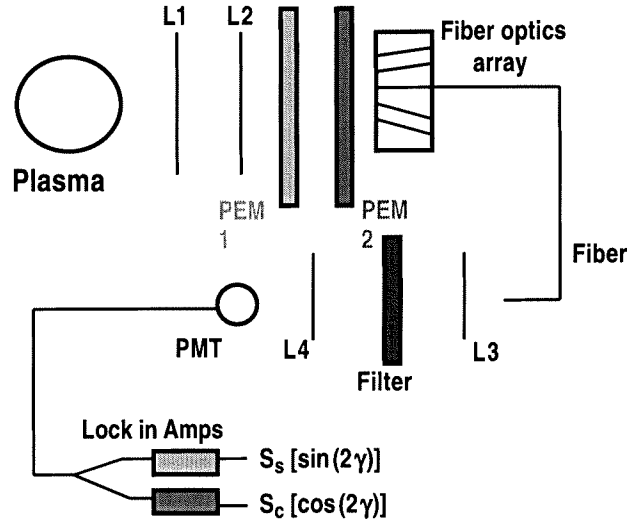


Fig. 2. Schematic of MSE diagnostic detection on DIII-D.

where I_{σ} and I_{π} are the intensities of the σ and the π polarizations, I_{bk} is the intensity of background light, γ is the polarization angle being measured, and ω_1 and ω_2 are the two modulation frequencies of the PEMs. The light is then focused onto fibers that are routed to the detection electronics for each channel. The σ component of the spectrum is selected using an interference filter and detected with a photomultiplier tube. The filter also rejects the π to increase the signal-to-noise ratio. The spectrum is Doppler shifted depending upon the view chord and this helps in eliminating the D_{α} emission from other intersecting volumes and the background plasma. The photomultiplier output is split and fed into two lock-in detectors operating synchronously at the frequencies, $2\omega_1$ and $2\omega_2$. The lock-in output voltages, S_s and S_c , are the signals proportional to the sine and the cosine of twice the polarization angle [Eq. (2)]. Taking into account instrument responses, offsets and sensitivity of the optics to magnetic field, the MSE pitch angle can be obtained from the ratio of the lock-in signals from the relation

$$\gamma = \frac{1}{c_1} \left[\frac{1}{2} \tan^{-1} \left(\frac{S_s}{c_2 S_c} \right) - (c_3 + c_4 B_t) \right] \quad (3)$$

where c_1 , c_2 , c_3 , and c_4 are calibration constants unique to each channel and B_t is the toroidal magnetic field.

For MHD modes, the assumption of a constant radial electric field (in time) may be a reasonable one, but requires confirmation. Also, for tokamaks, the variations in toroidal field from vacuum values is small. With these assumptions, the poloidal field oscillation (oscillation in B_z) associated with a rotating MHD mode is proportional to the oscillation in pitch angle, or $B_z \sim (A_2/A_1)\gamma \tilde{B}_t$, where the sign \sim refers to the oscillating component.

3. MEASUREMENT OF PERTURBED MAGNETIC FIELD DUE TO A RESISTIVE WALL MODE

When the plasma pressure, specifically the normalized β , $\beta_N = 100\beta_t (\%) [aB_t/I]$ exceeds plasma stability limit with no stabilizing wall, the plasma exhibits a kink mode. Here $\beta_t =$ toroidal $\beta = 2\mu_0\langle p\rangle/B_t^2$, $\langle p\rangle$ is the volume averaged plasma pressure, I is the plasma current in MA and a is the plasma minor radius in m. In the absence of a nearby wall, the plasma is subject to a fast-growing instability. If there is a resistive wall near the plasma boundary, the kink mode couples to the wall and a relatively slowly growing mode, the RWM, appears. The DIII-D tokamak has internal [6] and external coils to control the RWM through feedback techniques.

A different application uses the internal coils as antennae for active MHD spectroscopy [7]. The coils are energized with a three-phase rotating current and with relative phasing arranged to produce a helical field rotating at frequencies of the order of 10 Hz. The slowly rotating field applied by the internal coils excites a stable RWM to a finite amplitude and causes it to rotate synchronously with the applied field. Figure 3 shows the signals for the β_N , the no-wall β_N limit, the plasma toroidal rotation velocity, the internal coil current and the radial response seen by coil probe outside the vessel wall as a function of time. Once the plasma β_N crosses the no-wall limit, the RWM is close to marginal stability. At a later time, an alternating current is applied to the internal coils [Fig. 3(c)] and the radial field from the RWM shows a finite amplitude response [Fig. 3(d)].

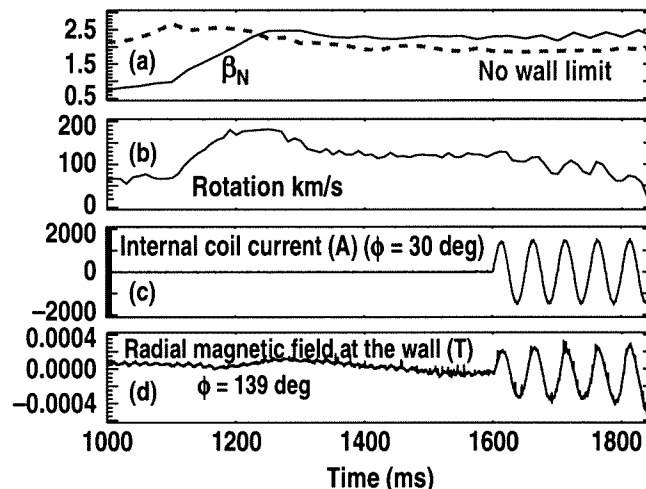


Fig. 3. Conditions of the plasma discharge during the presence of RWM and the internal coil current which rotates the mode (Shot 113550).

Figure 4 shows that the magnetic field perturbation due to the rotating RWM is observed in the motional Stark effect diagnostic signal. The pitch angle oscillation (after subtracting the average pitch angle) for the channel at $R = 2.04$ m is shown along with a similar response of electron temperature as measured by the ECE diagnostic for a channel at $R = 2.05$ m. These represent the sum of the applied field perturbation and the resonant plasma response, which is the dominant quantity. The internal coil current, alternating at 20 Hz, is also shown again for reference. The plots show that the MSE pitch angle (approximately proportional to B_z) oscillates due to the rotating mode as does the electron temperature. The pitch angle oscillations are observed on all MSE channels viewing different plasma radii. The Fourier transform of the pitch angle signal gives the amplitude of the oscillation at 20 Hz. The radial profile of the amplitude of the oscillating component of the B_z ($= B_{\text{poloidal}}$ at the observation plane $z = 0$), obtained from the pitch angle amplitudes of different MSE channels, is shown in Fig. 5. The profile is normalized to the RMS amplitude of 85 G. The corresponding profile of the amplitude of electron temperature oscillation (normalized to 65 eV) also shows a very similar profile indicating that the mode is present over much of the plasma. The perturbation profile is peaked near the location where the tokamak safety factor $q \sim 2$ — this is consistent with RWM models. The flux surface displacement can be estimated from the relation $\xi \sim (B_z/B)R$. This gives a RMS displacement value of ~ 0.55 m, which is in good agreement with that obtained from the ECE measurements [$\xi = Te/(dTe/dr)$] of ~ 0.5 cm.

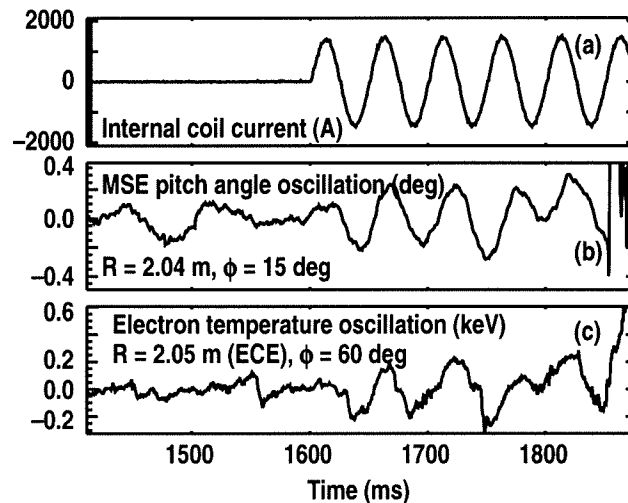


Fig. 4. Internal coil current and the oscillating signals on the MSE channel and ECE channels. The MSE and ECE signals have been smoothed to remove high frequency noise (Shot 113550).

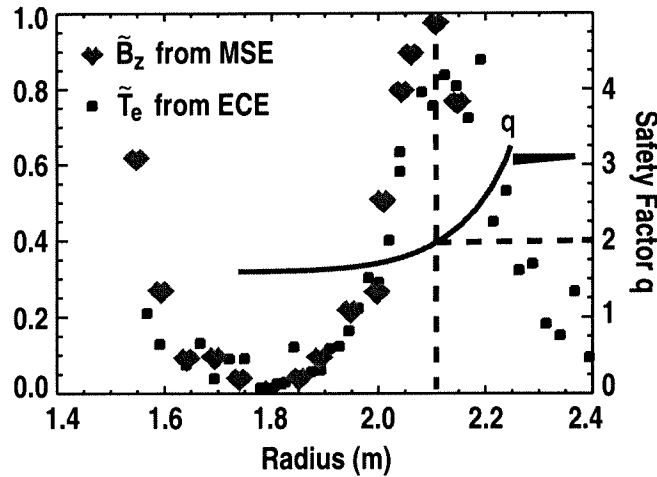


Fig. 5. Radial profile of the normalized amplitudes of oscillating components of the poloidal field (from MSE) and electron temperature (from ECE) (Shot 113550).

Soft x-ray measurements which are available at two toroidal locations show that there is a strong $n=0$ component in addition to the RWM which has a toroidal mode number of $n=1$. The above measurements of the perturbed poloidal field of the RWM and the electron temperature include both the $n=0$ and $n=1$ components. Comparison with other diagnostics shows that the amplitude of the two modes are comparable. Further studies on resolving the measurement and the underlying physics are in progress.

Such a measurement has not been previously done for an MHD instability and, for the first time, these measurements will give the detailed structure information that can now be compared with stability model predictions.

4. MEASUREMENT OF MHD ACTIVITY WITH HIGH FREQUENCY

The above technique of measuring the MHD amplitude is applicable only when the observed frequency of the mode is much smaller than the modulation frequency of the PEMs used for the MSE diagnostic. Typically, the PEM frequencies tend to be around 20 kHz for a large aperture optical arrangement and, therefore, modes with frequencies <5 kHz may be observed. For MHD modes which have higher frequencies in the observation frame, such as rotating tearing or interchange modes or high frequency electromagnetic activity, a new approach has been devised and reported in this paper.

With instrument responses taken into account and including the oscillating component of the different parameters, Eq. (2) for the total MSE intensity can be written as

$$I_{\text{tot}} = I + \tilde{I} \cos(\omega t) + \left[A_s + \tilde{A}_s \cos(\omega t) \right] \cos(\omega_s t) \sin \left[2(\gamma + \tilde{\gamma} \cos(\omega t)) \right] \\ + \left[A_c + \tilde{A}_c \cos(\omega t) \right] \cos(\omega_c t) \cos \left[2(\gamma + \tilde{\gamma} \cos(\omega t)) \right] + \dots \quad (4)$$

where A_s and A_c are the amplitudes of the MSE instrument signals associated with the $\sin(2\gamma)$ and $\cos(2\gamma)$ terms respectively and $\omega_s = 2\omega_1$ and $\omega_c = 2\omega_2$. The superscript \sim refers to the component of the parameter that is oscillating at a frequency ω . The oscillating components intensities (\tilde{I} and the \tilde{A}_s) are associated with oscillations of the plasma density and/or the diagnostic neutral beam density. With the assumption that the oscillating component of γ is small, the signals corresponding to the $\sin(2\gamma)$ and $\cos(2\gamma)$ terms can be simplified to

$$S_s = A_s \cos(\omega_s t) \sin(2\gamma) + \frac{\cos[(\omega_s + \omega)t] + \cos[(\omega_s - \omega)t]}{2} \left[\tilde{A}_s \sin(2\gamma) + 2A_s \tilde{\gamma} \cos(2\gamma) \right] \\ S_c = A_c \cos(\omega_c t) \cos(2\gamma) + \frac{\cos[(\omega_c + \omega)t] + \cos[(\omega_c - \omega)t]}{2} \left[\tilde{A}_c \cos(2\gamma) - 2A_c \tilde{\gamma} \sin(2\gamma) \right] \quad (5)$$

From these expressions, one obtains the relations for the oscillating component of the pitch angle and signal amplitudes as

$$\tilde{\gamma} = \frac{R_s - R_c}{\cot(2\gamma) + \tan(2\gamma)} = 0.5(R_s - R_c) \sin(4\gamma) \\ \frac{\tilde{A}_s}{A_s} = \frac{\tilde{A}_c}{A_c} = 2R_s - \tilde{\gamma} \cot(2\gamma) = 2 \left[R_s \sin^2(2\gamma) + R_c \cos^2(2\gamma) \right] \quad (6)$$

With

$$R_s = \frac{S_{\omega_s - \omega}}{S_{\omega_s}} = \frac{\tilde{A}_s \sin(2\gamma) + 2A_s \tilde{\gamma} \cos(2\gamma)}{A_s \sin(2\gamma)}$$

$$R_s = \frac{S_{\omega_c + \omega}}{S_{\omega_c}} = \frac{\tilde{A}_s \sin(2\gamma) + 2A_s \tilde{\gamma} \cos(2\gamma)}{A_s \sin(2\gamma)}$$

The signals at the frequencies $(\omega_s + \omega)$ and $(\omega_c - \omega)$ are also related in a same fashion. In addition, the oscillating component of the plasma density and beam density product can be obtained from the oscillating component at the frequency ω . In the above derivations, though the relationships are simplified by the assumption of no phase difference between the MHD oscillations and the PEM modulation, more general derivations give similar results. Also, the assumption has been made that there is no phase difference between density perturbations and B_z perturbations. It must be noted that $R_s - R_c$ is much smaller than R_s or R_c and, therefore, the signal analysis has to be carried out with high accuracy to obtain the correct value of the perturbed pitch angle. The use of the signal at the mode frequency (ω) is being evaluated to improve the sensitivity.

The above analysis was applied to new measurements on a rotating tearing mode in the DIII-D tokamak. Figure 6 shows the results of the mode analysis of the signals from magnetic (Mirnov) probe s at the wall. Again, this measurement is a first ever measurement of the local

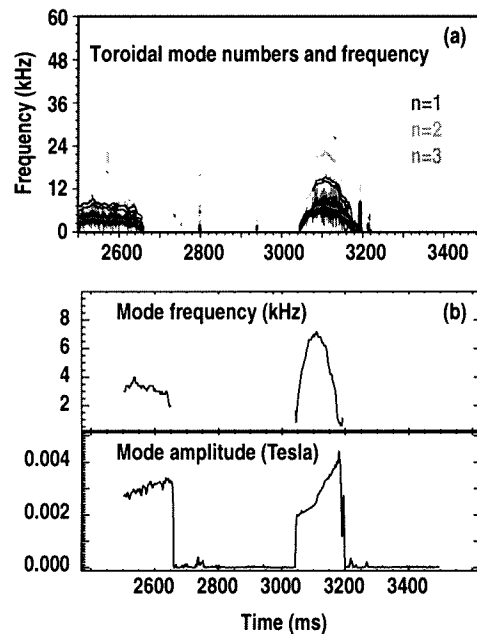


Fig. 6. Results from the analysis of magnetic probe signals (a) this shows that there is only one mode (with toroidal mode number $n=1$) (b) frequency and amplitude of the $n=1$ mode (Shot 114712).

magnetic field perturbation associated with an MHD mode. Figure 6(a) shows that there is an $n=1$ mode at $t \sim 2500$ ms, and another at $t \sim 3100$ ms. Figure 6(b) shows the frequency and amplitude of perturbed poloidal field (at the wall) of the $n=1$ mode. The poloidal mode number of this tearing mode m is likely to be 2, since it is located near the surface where the safety factor value is 2. The photomultiplier signal of the MSE channel at $R = 2.14$ m was digitized at 1 MHz and a spectrum analysis was carried out. Figure 7(a) shows the contours of power spectrum of the MSE signal. Figure 7(b) shows the same spectrum at 2900 to 3300 ms for clarity. (The tokamak equilibrium and flux contours for this discharge and the location of this measurement are shown in Fig. 8). The feature at ~ 40 kHz corresponds to $\omega_s/2\pi$ and the feature at ~ 46 kHz corresponds to $\omega_c/2\pi$. The other features are at the frequencies $\omega_1/2\pi$ and $\omega_2/2\pi$, the beat frequency $(\omega_1 - \omega_2)$ and various other beat frequencies of the PEM modulation.

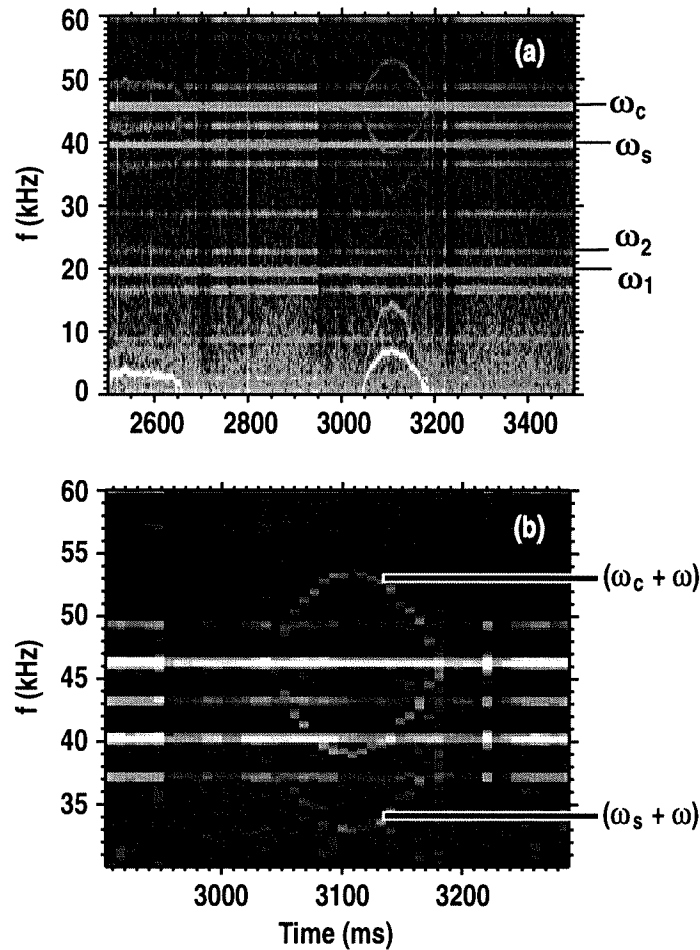


Fig. 7. Power Spectrum of the MSE signal at $R = 2.14$ m. (a) Spectrum showing modes at $t \sim 2500$ to 2650 ms and $t \sim 3050$ to 3200 ms. (b) Closer view of the spectrum at $t \sim 3050$ to 3200 ms (Shot 114712).

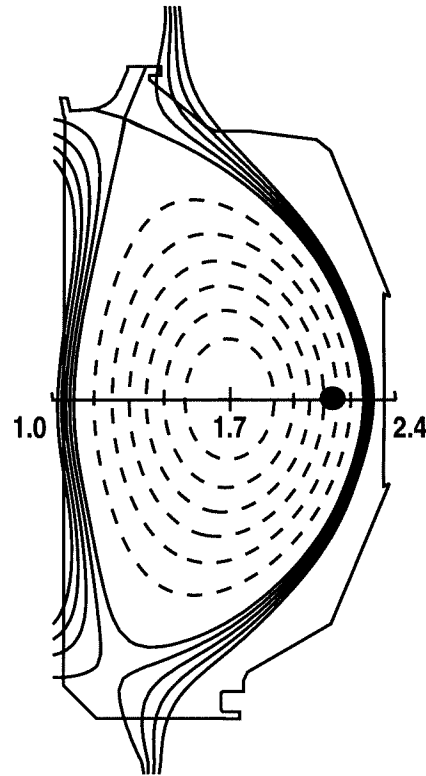


Fig. 8. Plasma equilibrium at $t \sim 3000$ ms and poloidal flux contours. The major radius and x marks the location of the measurement by the MSE channel (Shot 114712).

In addition to these basic frequencies produced by PEM modulation of the polarized light, one can also clearly see the beat frequencies $(\omega_s - \omega)/2\pi$, $(\omega_c + \omega)/2\pi$, $(\omega_s + \omega)/2\pi$ and $(\omega_c - \omega)/2\pi$. For example, the peaks at ~ 47 kHz and ~ 54 kHz at 3100 ms are the beat frequencies $(\omega_s + \omega)/2\pi$, $(\omega_c + \omega)/2\pi$ with the mode amplitude whose frequency is about ~ 7 kHz. This is a phase of the plasma where the plasma rotation is rapidly changing and the observed mode frequency is well correlated with the rotation. With this rapid variation in mode frequency, this phase is very useful to illustrate the efficacy of the MSE measurement. It can be seen that this straight forward spectral analysis of the MSE raw signals shows the same structure as the Mirnov signals and also the response at various beat frequencies at all times. There is also a clear signal at the fundamental mode frequency ω as indicated by Eq. (4) due to the oscillation of the total intensity due to density fluctuations. The mode frequency and the beat frequencies are in excellent agreement with the Mirnov signals. The frequencies are also in excellent agreement with the results of the spectrum analysis of ECE signals viewing at $R = 2.1$ m (Fig. 9). One other channel at $R = 2.21$ m from the same MSE array, does not register the MHD mode, showing that the measurement at $R = 2.14$ m is a local measurement.

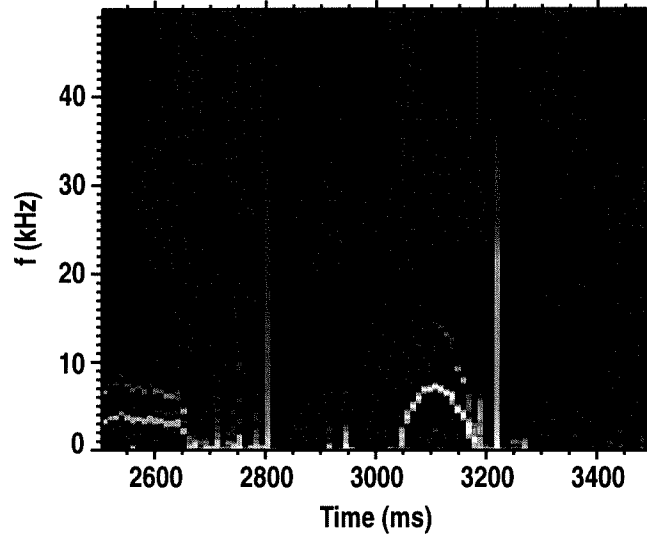


Fig. 9. Spectrum of electron temperature fluctuations as a function of time (Shot 114712).

The amplitude spectrum is plotted for the time slice ~ 3100 ms in Fig. 10 when a mode is present (magenta) and compared with the spectrum at ~ 3010 ms (blue) when there is no mode. As in the power spectrum contour plot, the MHD-induced pitch angle oscillation can be clearly seen. The signals have been analyzed using the above formulation for this channel data. Using the observed amplitudes at the desired frequencies and using Eq. (6), the following results are

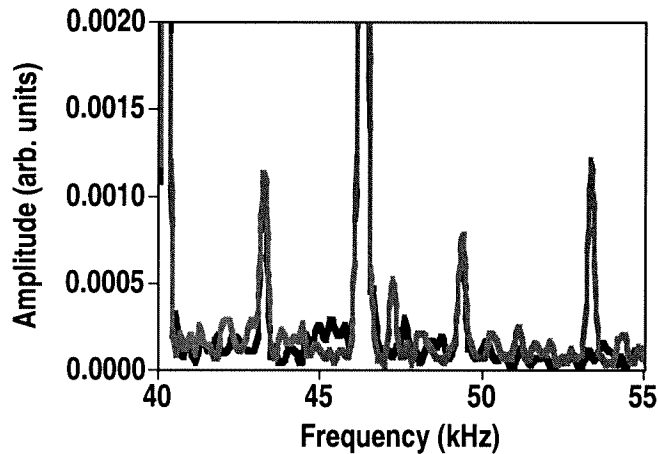


Fig. 10. Spectrum from the MSE signal for two time slices. Blue represents $t \sim 3010$ ms when the tearing mode is not present. Magenta represents $t \sim 3100$ ms when the tearing mode is present (Shot 114712).

obtained at the time slice of $t = 3100$ ms, $\omega_c = 46.4$ kHz, $\omega_s = 40.3$ kHz and $\omega = 6.9$ kHz. The signals at frequencies 33.2, 40.3, 46.4 and 53.5 kHz give $R_s = 0.141$ and $R_c = 0.134$ and therefore $\tilde{\gamma} = 0.16$ deg (peak to peak) corresponding to a RMS oscillating poloidal field \tilde{B}_z of

~83 G. This is in good agreement with the magnetic probe data shown in Fig. 6(b). The magnetic perturbation is expected to vary as $B_{\sim} \sim 1/r^{m+1} \sim 1/r^3$. With $R(\text{axis}) = 1.72$ m; $R(\text{MSE}) = 2.14$ m and $R(\text{wall}) \sim 2.4$ m, the value of 83 G at the MSE observation location gives an estimated value at the wall ~21 G, which is in excellent agreement with the probe measurement of ~23 G. The modes at 2500 ms and at 3100 ms are likely to be tearing modes, since interchange $n=1$ modes with large amplitudes are not observed in the outer edge of the plasma. Multi-channel measurements are being carried out to obtain the spatial and temporal characteristics of such modes.

5. CONCLUSIONS

The local plasma oscillating component of the poloidal field associated with MHD mode in a hot plasma has been detected for the first time using the MSE diagnostic. The radial structure of the magnetic perturbation associated with a RWM rotating at 20 Hz was obtained using standard MSE detection. A rotating tearing mode, with an observed frequency of up to 7 kHz, was detected using a newly devised technique of digitizing MSE signals at a fast rate and relating the spectral analysis results to obtain the perturbed pitch angle and, therefore, the perturbed poloidal field. These observations demonstrate that the MSE diagnostic can be used for observing high frequency phenomena which give rise to magnetic fluctuations in the observer frame such as MHD instabilities and electromagnetic turbulence. Additional channels and signal analysis capabilities are being added in the DIII-D tokamak to obtain the structure of MHD modes and to extend the measurement sensitivity and applicability to a wide range of frequencies.

ACKNOWLEDGMENT

This work supported by the U.S. Department of Energy under Contract Nos. DE-AC03-99ER54463, W-7405-ENG-48, and Grant Nos. DE-FG03-97ER54415, DE-FG02-89ER53297, DE-FG03-01ER54615.

REFERENCES

- [1] D. Wroblewski, L.L. Lao, Rev. Sci. Instrum. **63**, 5140 (1992).
- [2] B.W. Rice, K.H. Burrell, L.L. Lao, Y.R. Lin-Liu, Phys. Rev. Lett. **79**, 2694 (1997).
- [3] B.W. Rice, D.G. Nilson, K.H. Burrell, L.L. Lao, Rev. Sci. Instrum. **70**, 815 (1999).
- [4] F.M. Levinton, Phys. Rev. Lett. **63**, 2060 (1989).
- [5] A.M. Garofalo, T.H. Jensen, L.C. Johnson, R.J. La Haye, G.A. Navratil, M. Okabayashi, J.T. Scoville, E.J. Strait, D.R. Baker, J. Bialek, M.S. Chu, J.R. Ferron, J. Jayakumar, L.L. Lao, M.A. Makowski, H. Reimerdes, T.S. Taylor, A.D. Turnbull, M.R. Wade, S.K. Wong, Phys. Plasmas **9**, 1997 (2002).
- [6] G.L. Jackson, P.M. Anderson, J. Bialek, W.P. Cary, G.L. Campbell, A.M. Garofalo, R. Hatcher, A.G. Kellman, R.J. La Haye, A. Nagy, G.A. Navratil, M. Okabayashi, C.J. Pawley, H. Reimerdes, J.T. Scoville, E.J. Strait, D.D. Szymanski, "Initial Results from the New Internal Magnetic Field Coils for Resistive Wall Mode Stabilization in the DIII-D Tokamak," to be published in *Proceedings of the 30th European Physical Society Meeting*, St. Petersburg, Russia, 2003.
- [7] H. Reimerdes, M.S. Chu, A.M. Garofalo, G.L. Jackson, T.H. Jensen, R.J. La Haye, G.A. Navratil, M. Okabayashi, J.T. Scoville, E.J. Strait, "Resistive Wall Modes and Plasma Rotation in DIII-D," to be published in *Proceedings of the 30th European Physical Society Meeting*, St. Petersburg, Russia, 2003.
- [8] J.C. Kemp, J. Opt. Soc. Am. **59**, 950 (1969).